THE ASTRONOMICAL JOURNAL VOLUME 89, NUMBER 7 JULY 1984

SIDEDNESS, FIELD CONFIGURATION, AND COLLIMATION OF EXTRAGALACTIC RADIO JETS

ALAN H. BRIDLE
National Radio Astronomy Observatory,[a] Charlottesville, Virginia 22901
Received 27 February 1984; revised 26 March 1984

ABSTRACT

Data on 125 extragalactic radio jets are used to show that those in sources with total powers $\lesssim 10^{24.5}$ W/Hz at 1.4 GHz (or, equivalently, core powers $< 10^{23}$ W/Hz at 5 GHz) are generally two sided and dominated by perpendicular magnetic field components over most of their lengths. In contrast, those in sources with larger total and core powers are generally one sided and dominated by parallel magnetic field components over most of their lengths. The resolved jets in the weaker sources generally have faster lateral expansion (spreading) rates than those in the more powerful sources.

I. INTRODUCTION

This paper emphasizes three characteristics of jets in radio galaxies and QSR's which correlate with the core and total radio powers of the sources. These characteristics are (a) their sidedness, (b) their (large-scale) apparent magnetic field configurations, and (c) their lateral expansion (spreading) rates. The first two correlations were previously noted in a sample of 69 jetted extragalactic sources examined by Bridle (1982). They are confirmed and extended here using data from a list of 125 such sources compiled by Bridle and Perley (1984, henceforth BP) from observations with the VLA, MERLIN, and the WSRT, and with VLB arrays.

The BP list comprises all extragalactic sources known to its authors in mid-August 1983 to contain a radio "jet" that is (a) at least four times as long as it is wide, (b) separable at high resolution from other extended structures (if any) either by brightness contrast or spatially, and (c) aligned with the compact radio core where it is closest to it. The BP list is not statistically "complete" to a given flux-density limit, or in a given volume of space. It is, however, the largest available catalog of jets in sources representing the entire $\sim 10^7$:1 range of total radio powers associated with active extragalactic objects. This paper discusses three trends present in this representative jet list that are very unlikely to be artifacts of statistical incompleteness in it.

II. SIDEDNESS

a) The Definition of Sidedness Ratio

The term *sidedness ratio* (S) is used here to connote the ratio of intensities per synthesized beam between the brighter and fainter radio jets in a radio galaxy or QSR, measured at the same separation from the core on opposite sides of the parent object and *at low resolution transverse to the jets*. The resolution restriction is made to ensure that S measures ratios of radiated power between a jet and its counterjet without confusion by differences in their lateral expansion rates or transverse intensity profiles.

b) Practical Difficulties

Sidedness ratios between jets and their counterjets vary from unity to several hundreds from object to object. They may also vary with distance from the unresolved core in the same object, as in NGC 6251 (Perley *et al.* 1984). Estimates of S along jets without detected counterjets are limited by the finite dynamic range (DR) and sensitivity of radio maps. Self-calibration (e.g., Schwab 1980; Pearson and Readhead 1984) of data from imaging radio-telescope arrays often produces maps with DR's > 1000:1, but much of this DR can be "used up" detecting the jets at all in the presence of bright radio cores. In many cases, the best available self-calibrated maps set limits to S that are only from 4:1 to 10:1. Unless the counterjet is also detected, limits to S vary along blobby jets in ways that reflect only the finite DR of the map and not actual variations in S. It is therefore difficult to use S as a continuous, unbiased parameter for jet asymmetries.

It is also difficult to quantify jet sidedness if the intensity asymmetries may be the result of Doppler boosting of the approaching sides of two-sided bulk relativistic flows close to the line of sight. The "corresponding" regions of a jet and its counterjet would not then appear equidistant from the central cores. Their sidedness ratio should be measured between points whose locations depend both on the bulk Lorentz factors of the jet flows and (if they are not straight) on their detailed shapes and on their dynamics. The correspondence between regions on the two sides of the source cannot be established uniquely unless the counterjet is detected. This difficulty cannot be bypassed by using ratios of integrated jet and counterjet intensities: the areas of sky over which the jet and counterjet intensities should be integrated also depend on the bulk Lorentz factors and shapes of the jets, and on the (sometimes different) ways in which the jet and counterjet terminate to form lobes. If the counterjet is entirely or partially undetected, the shapes and sizes of the appropriate integration regions are unclear. Even without these complications for relativistic jets, "integrated" sidedness ratios for one-sided jets are very sensitive to the number of beamwidths along the detected jet and to the statistics of the fluctuations (noise and sidelobes) on the map.

All of the above problems will remain until maps with still higher DR detect counterjets in most sources. For the time being, I therefore simply bin S into three groups, recognizing the limitations of the presently available data: *one-sided* jets (or segments of jets) are those for which S is more than 4:1 everywhere that the DR of the map allows this to be determined, and *two-sided* jets are those for which it is less than 4:1 everywhere that the brighter jet can be detected. Those few cases for which the above categorization varies with distance from the core (usually around an S of about 4:1) are classified as "transitional." The break point is set at $S = 4$:1 solely because this choice leads to a classification that can be

[a] The National Radio Astronomy Observatory is operated by Associated Universities, Inc., under contract with the National Science Foundation.

 0004-6256/84/070979-08$00.90

TABLE I. Power and sidedness data for 94 jets.

Source Name(s)		ID, z	$\log_{10} P^{5}_{\rm core}$	$\log_{10} P^{1.4}_{\rm tot}$	SID	L_j (kpc)
0017 + 15	= 3C9	Q, 2.0120	25.45	28.16	1	30
0055 + 30	= NGC 315	G, 0.0167	23.24	24.08	T	240
0055 + 26	= NGC 326	G, 0.0472	22.29	24.61	2	25
0104 + 32	= 3C31	G, 0.0169	22.45	24.21	2	14
0106 + 72	= 3C33.1	G, 0.1810	23.76	26.11	1	140
0123 − 01	= 3C40	G, 0.0186	22.35	24.38	2	38
0206 + 35	= UGC 1651	G, 0.0373	23.15	24.52	2	18
0220 + 42	= 3C66B	G, 0.0215	22.59	24.69	2	45
0238 + 08	= NGC 1044	G, 0.0214	22.54	23.80	2	43
0240 − 00	= 3C71	G, 0.0040	20.99	22.94	2	0.29
0255 + 05	= 3C75A,B	G, 0.0241	22.40	24.61	2	30
0256 + 13	= 4C13.17B	G, 0.0748	22.30	24.07	2	15
0305 + 03	= 3C78	G, 0.0289	23.77	24.83	1	0.60
0314 + 41	= NGC 1265	G, 0.0255	22.15	24.76	2	18
0316 + 41	= NGC 1275	G, 0.0177	24.87	24.66	1	5.0
0320 − 37	= For A	G, 0.0063	21.23	24.69	T	2.7
0326 + 39	= B2	G, 0.0243	22.70	24.06	2	41
0336 − 35	= NGC 1399	G, 0.0049	20.41	22.71	2	8.1
0415 + 37	= 3C111	G, 0.0485	24.47	25.59	1	78
0430 + 05	= 3C120	G, 0.0334	24.93	24.76	1	83
0445 + 44	= 3C129	G, 0.0208	22.19	24.58	T	8.8
0449 − 17	= PK	G, 0.0313	22.03	23.93	2	10
0459 + 25	= 3C133	G, 0.2775	25.33	26.72	1	14
0514 − 16	= PK	Q, 1.2780	27.32	27.25	1	33
0538 + 49	= 3C147	Q, 0.5450	26.78	27.95	1	0.77
0658 + 33	= B2	G, 0.1270	23.98	24.82	2	55
0704 + 35A	= 4C35.16A	G, 0.0780	21.83	24.28	2	17
0723 + 67	= 3C179	Q, 0.8460	26.62	27.39	1	18
0742 + 31	= 4C31.30	Q, 0.4620	26.24	26.55	1	210
0812 + 36	= B2	Q, 1.0250	27.10	27.23	1	30
0824 + 29	= 3C200	G, 0.4580	24.98	26.73	1	41
0833 + 65	= 3C204	Q, 1.1120	25.71	27.39	1	52
0838 + 13	= 3C207	Q, 0.6840	26.45	27.23	1	25
0855 + 14′	= 3C212	Q, 1.0490	25.38	27.61	1	22
0908 + 37	= B2	G, 0.1040	23.50	24.89	2	23
0917 + 45	= 3C219	G, 0.1744	24.18	26.45	1	36
0938 + 39	= 4C39.27	Q, 0.6180	25.00	26.99	1	96
0957 + 56	=	Q, 1.4050	26.28	27.15	1	21
1003 + 35	= 3C236	G, 0.0989	24.64	25.78	1	0.37
1004 + 14	= NGC 3121	G, 0.0310	22.97	24.07	2	77
1004 + 13	= 4C13.41	Q, 0.2400	23.87	25.92	1	60
1007 + 41	= 4C41.21	Q, 0.6130	25.86	26.91	1	77
1029 + 57	= HB13	G, 0.0340	22.50	23.70	2	280
1100 + 77	= 3C249.1	Q, 0.3110	25.00	26.41	1	21
1122 + 39	= NGC 3665	G, 0.0067	20.46	21.76	2	3.9
1131 + 49	= IC 708	G, 0.0321	22.74	24.13	2	35
1137 + 18	= NGC 3801	G, 0.0105	20.59	23.06	2	2.1
1150 + 49	= 4C49.22	Q, 0.3340	25.88	26.43	1	23
1209 + 74	= 4CT74.17.1	G, 0.1070	23.26	24.99	1	120
1216 + 06	= 3C270	G, 0.0073	22.25	24.01	2	31
1222 + 13	= 3C272.1	G, 0.0051	21.72	23.24	2	3.3
1226 + 02	= 3C273	Q, 0.1580	26.92	27.12	1	39
1228 + 12	= Vir A	G, 0.0051	22.92	24.78	1	1.8
1250 − 10	= NGC 4760	G, 0.0138	22.14	23.27	2	2.9
1251 + 278	= 3C277.3	G, 0.0857	22.98	25.37	1	11
1251 − 12	= 3C278	G, 0.0138	22.13	24.23	2	14
1253 − 05	= 3C279	Q, 0.5360	27.56	27.53	1	9.9
1258 + 40	= 3C280.1	Q, 1.6590	26.21	27.84	1	42
1315 + 34	= B2	Q, 1.0500	26.76	26.98	1	13
1321 + 31	= NGC 5127	G, 0.0161	21.77	23.85	2	55
1322 − 42	= Cen A	G, 0.0012	22.20	24.62	1	5.2
1333 − 33	= IC 4296	G, 0.0129	22.46	24.05	2	130
1407 + 17	= NGC 5490	G, 0.0163	22.00	23.68	2	5.5
1414 + 11	= 3C296	G, 0.0237	22.67	24.43	2	50
1448 + 63	= 3C305	G, 0.0410	22.57	24.73	2	0.94
1450 + 28	= B2	G, 0.1265	22.56	24.56	2	37
1451 − 37	= PK	Q, 0.3140	26.24	26.36	1	17
1615 + 42		G, 0.1310	23.20	24.20	2	14
1626 + 27	= 3C341	G, 0.4480	23.49	26.80	T	110
1637 + 82	= NGC6251	G, 0.0230	23.66	24.14	1	160
1638 + 53	= 4C53.37	G, 0.1098	23.21	24.93	2	40
1641 + 39	= 3C345	Q, 0.5940	27.62	27.52	1	9.5
1648 + 05	= 3C348	G, 0.1540	23.61	27.10	1	120
1752 + 32	= B2	G, 0.0449	22.67	23.46	2	30
1807 + 69	= 3C371	G, 0.0500	24.60	24.84	1	2.0

TABLE I. (continued).

Source Name(s)		ID, z	$\log_{10} P^{5}_{\rm core}$	$\log_{10} P^{1.4}_{\rm tot}$	SID	L_j (kpc)
1842 + 45	= 3C388	G, 0.0908	23.76	25.73	1	18
1857 + 56	= 4C56.28	Q, 1.5950	26.34	27.57	1	62
1919 + 47	= 4C47.51	G, 0.1030	23.19	24.86	1	265
1939 + 60	= 3C401	G, 0.2010	24.14	26.37	1	24
1940 + 50	= 3C402N	G, 0.0247	22.08	24.31	2	6.2
2037 + 51	= 3C418	Q, 1.6860	28.24	28.41	1	9.3
2116 + 26	= NGC 7052	G, 0.0164	22.12	22.72	2	25
2153 + 37	= 3C438	G, 0.2920	23.99	26.86	2	27
2221 − 02	= 3C445	G, 0.0570	23.51	25.30	1	210
2229 + 39	= 3C449	G, 0.0171	22.07	24.03	2	19
2236 + 35	= B2	G, 0.0277	21.88	23.40	2	7.7
2251 + 15	= 3C454.3	Q, 0.8590	28.02	28.10	1	21
2300 − 18	= PK	Q, 0.1290	24.90	25.45	1	68
2316 + 18	= OZ127	G, 0.0395	22.41	23.70	2	16
2318 + 07	= NGC 7626	G, 0.0112	21.31	23.17	2	6.4
2335 + 26	= 3C465	G, 0.0293	23.37	24.85	1	24
2337 + 26	= NGC 7728	G, 0.0314	23.15	23.49	2	39
2349 + 32	= 4C32.69	Q, 0.6710	25.15	26.57	1	98
2354 + 47	= 4C47.63	G, 0.0460	22.49	24.63	T	37

applied to about 3/4 of the available jet maps, while a break at a higher ratio could not. The classification reveals a good correlation between sidedness and source power, but I do not imply that $S = 4{:}1$ reflects a threshold with particular physical significance.

c) Jet Sidedness and Source Power

Table I lists parameters for the 94 sources of the 125 in the BP list (a) whose jet sidedness can be classified using the above scheme from maps available to me and (b) whose redshifts are known. Column 1 gives the source name and column 2 its optical identification and redshift. Columns 3 and 4 give the logarithm of the core power in W/Hz at 5 GHz ($P^{5}_{\rm core}$) and of the total source power in W/Hz at 1.4 GHz ($P^{1.4}_{\rm tot}$), assuming $H = 100$ km s^{-1} Mpc^{-1} and an Einstein-de Sitter cosmology. The frequencies at which these powers are derived are chosen for observational convenience. Core flux densities are most often available (and least likely to be contaminated by inner jet emission) when measured on high-resolution synthesis maps at 5 GHz, while total flux densities are most often available (and least likely to be underestimated due to resolution) from single-dish studies at 1.4 GHz. For a few sources, the core flux density at 5 GHz or the total flux density at 1.4 GHz has been estimated using data from nearby frequencies, assuming spectral indices of 0.0 and 0.7 for the core and total emission, respectively; the uncertainties in flux densities estimated by these means are small in relation to the overall range of core and total powers, which is $> 10^{7}$:1.

Most of the 94 jets are one sided where they are closest to their parent object, be it a radio galaxy or a QSR. Most of those in weak radio galaxies quickly become two sided, whereas those in powerful radio galaxies and QSR's remain one sided over most (often all) of their length. Column 5 (SID) therefore codifies the sidedness *of the outer 90%* of the lengths of the jets (1 = one sided, 2 = two sided, T = transitional case). Column 6 gives the projected length of each jet in kpc.

Figure 1 shows a logarithmic plot of core power against total power, distinguishing different sidednesses of the outer 90% of the jets. The range in core and total powers is so large that the effects of K corrections on the plot are minor, and these corrections have not been applied. As jets can be classified as two sided from maps with lower DR or poorer sensitivity than those required to classify them as one sided, Fig. 1 does not illustrate the relative numbers of one-sided and two-sided jets in an unbiased sample. There would, however, be no observational impediment to detecting counterjets in any of the sources with one-sided jets if the sidedness ratios in these sources were actually $< 4{:}1$. *The rarity of two-sided jets in sources with core powers $> 10^{23.5}$ W/Hz at 5 GHz, or total powers $> 10^{25}$ W/Hz at 1.4 GHz, is clearly real.*

d) Commentary

The two weakest cores associated with one-sided jets are those in Cen A ($P^{5}_{\rm core} = 10^{22.20}$ W/Hz) and M87 ($P^{5}_{\rm core} = 10^{22.92}$ W/Hz). Both jets are short (M87—1.8 kpc; Cen A—5.2 kpc). Their lengths are comparable to, or shorter than, the one-sided *bases* of longer two-sided jets in other sources with similar total powers. The unusual feature of the M87 and Cen A jets may therefore not be their one sidedness, but rather the fact that they terminate in two-sided "inner lobes" instead of leading into two-sided "outer jets" extending 10 to 50 kpc beyond them. Note also that while all the QSR jets are one sided, radio-galaxy jets may be either one or two sided, depending on the radio power. (There are 14 radio galaxies in the sample which have one-sided jets > 10 kpc long.)

The numbers of one- and two-sided jets in this sample are approximately equal, as are the numbers of sources with total powers above and below 10^{25} W/Hz at 1.4 GHz. This equality does not, however, reflect the relative numbers of such sources in complete *volume-limited* samples. The steep luminosity function of extragalactic radio sources means that weak sources with two-sided jets greatly outnumber powerful sources with one-sided jets in volume-limited samples. The BP jet list in this sense overemphasizes powerful sources, as a result of the general bias towards strong sources from flux-limited surveys in the best available maps from imaging radio telescopes.

III. MAGNETIC CONFIGURATION

a) The Data

Detailed polarimetry is available for about 40 of the 125 radio jets listed by BP. The Faraday screens in front of the

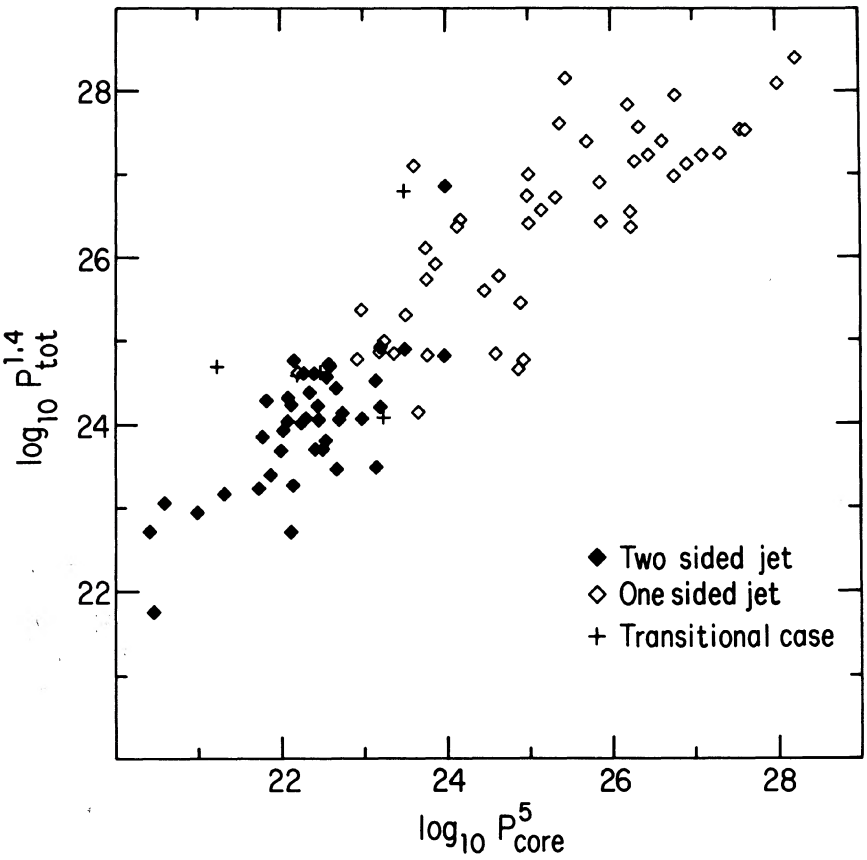

FIG. 1. Distribution of jet sidedness in the plane of logarithmic core power vs logarithmic total power, from the data in Table I.

jets have been mapped in detail only for a few (3C31, NGC 315, NGC 1265, M84, NGC 6251, and 3C449), but the known rotation measures (RM's) are rarely high enough to rotate 5-GHz E vectors by > 10 deg from their intrinsic (i.e., zero-wavelength) position angles *after correction for the integrated RM of the source*. The 5-GHz E vector data can therefore be used alone to estimate the apparent (synchrotron emissivity weighted) projected magnetic field configuration for most of these 40 jets with some confidence.

Three magnetic configurations occur frequently in well-resolved jets (BP)—the apparent B field may lie generally parallel to the jet axis, generally perpendicular to it, or be perpendicular at the center of the jet and parallel at its edges. Some jets whose low-level continuous emission is dominated by a parallel field have perpendicular or oblique fields at local bright knots (Perley *et al.* 1984; BP; Burns *et al.* 1984); these "local anomalies" (which may be due to oblique shocks in the jets) are disregarded here in favor of the underlying larger-scale field structure.

b) Field Configuration and Core Power

Table II lists the fraction $L_{\parallel}/L_j$ of the jet length L_j over which the parallel magnetic field component dominates *on the jet axis* for 38 jets in sources for which redshifts and the necessary polarimetry are both available. Figure 2 plots $L_{\parallel}/L_j$ against $\log_{10} P^5_{\rm core}$. Core power is chosen over total power arbitrarily for this plot; the plot is similar if total power is used as the independent variable. These data double the size of the sample discussed in this way by Bridle (1982), and confirm the trend in that smaller sample. In most sources with 5-GHz core powers $< 10^{23}$ W/Hz, the dominant component of the jet field quickly changes from parallel (near the core) to perpendicular. In contrast, parallel fields dominate virtually all along jets in sources with 5-GHz core powers $> 10^{24}$ W/Hz (neglecting local anomalies at bright knots as mentioned above).

c) Commentary

The initial parallel-field regimes of the jets in weak sources roughly coincide with their one-sided bases (Bridle 1982), though exceptions are known, e.g., 3C449 (Cornwell and Perley 1982) and NGC 1265 (C. P. O'Dea, private communication), in both of which the parallel-field regime is two sided. NGC 1265 has two-sided C-shaped jets in a "head-tail" structure that is dominated by a parallel field over much of its length. As parallel-field components are frequently enhanced on the outer edges of the bends in strongly curved jets (e.g., 3C31—Burch 1979; Strom *et al.* 1983; NGC 6251—Bridle and Perley 1983; Perley *et al.* 1984), some parallel-field segments of the outer jets in weak sources may arise by field stretching and shearing as a result of a strong interaction with an ambient medium. The jets in NGC 1265 may be an extreme example of this effect, wherein the trend to perpendicular-field dominance on the axis of a two-sided jet has been overcome by the viscous interaction with an external medium in a rich cluster. For this reason, jets in strongly bent head-tail sources are excluded from Table II and Fig. 2.

TABLE II. Power and magnetic configuration.

Source	$\log_{10}P^{5}_{\rm core}$	$\log_{10}P^{1.4}_{\rm tot}$	L_j (kpc)	$L_\parallel/L_j$
0017 + 15	25.45	28.16	30	1.0
0055 + 30	23.24	24.08	240	0.025
0055 + 26	22.29	24.61	25	0.087
0104 + 32	22.45	24.21	14	0.17
0106 + 72	23.76	26.11	140	1.0
0220 + 42	22.59	24.69	45	0.060
0326 + 39	22.70	24.06	41	0.092
0459 + 25	25.33	26.72	14	1.0
0732 + 67	26.62	27.39	18	1.0
0844 + 31	23.35	24.88	61	1.0
0917 + 45	24.18	26.45	36	1.0
0938 + 39	25.00	26.99	96	1.0
1004 + 13	23.87	25.92	60	0.68
1007 + 41	25.86	26.91	77	1.0
1137 + 18	20.59	23.06	2.1	0.14–0.38
1150 + 49	25.88	26.43	23	1.0
1209 + 74	23.26	24.99	120	1.0
1222 + 13	21.72	23.24	3.3	0.11
1226 + 02	26.92	27.12	39	0.96
1228 + 12	22.92	24.78	1.8	1.0
1253 − 05	27.56	27.53	9.9	1.0
1258 + 40	26.21	27.84	42	> 0.85
1317 + 52	26.79	27.37	60	1.0
1321 + 31	21.77	23.85	55	0.025
1322 − 42	22.20	24.62	5.2	0.18
1333 − 33	22.46	24.05	130	0.021
1414 + 11	22.67	24.43	50	0.017
1441 + 52	24.53	25.75	26	0.94
1618 + 17	25.78	26.97	63	1.0
1626 + 27	23.49	26.80	110	1.0
1637 + 82	23.66	24.14	160	0.18
1641 + 39	27.62	27.52	9.5	1.0
1648 + 05	23.61	27.10	120	1.0
1857 + 56	26.34	27.57	62	1.0
1939 + 60	24.14	26.37	24	1.0
2229 + 39	22.07	24.03	19	0.087
2251 + 15	28.02	28.10	21	1.0
2349 + 32	25.15	26.57	98	1.0

TABLE III. Mean lateral expansion rates.

Source	$\log_{10}P^{5}_{\rm core}$	$\log_{10}P^{1.4}_{\rm tot}$	$\overline{\Phi/\Theta}$
0055 + 30	23.24	24.08	0.11
0104 + 32	22.45	24.21	0.29
0106 + 72	23.76	26.11	0.06
0326 + 39	22.70	24.06	0.235
0415 + 37	24.47	25.59	0.04
0445 + 44	22.19	24.58	0.13
0917 + 45	24.18	26.45	0.07
1209 + 74	23.26	24.99	0.12
1226 + 02	26.92	27.12	0.013
1228 + 12	22.92	24.78	0.07
1258 + 40	26.21	27.84	0.05
1321 + 31	21.77	23.85	0.275
1322 − 42	22.20	24.62	0.19
1414 + 11	22.67	24.43	0.16
1637 + 82	23.66	24.14	0.08
1957 + 40	24.12	27.73	0.03
2229 + 39	22.07	24.03	0.20
2349 + 32	25.15	26.57	0.06

IV. COLLIMATION

a) Measuring Collimation

The rates at which transverse widths of well-resolved jets grow with increasing distance from the unresolved cores generally vary with distance (e.g., 3C31—Bridle *et al.* 1980; NGC 315—Willis *et al.* 1981; Bridle 1982; Cen A—Burns *et al.* 1983; NGC 6251—Saunders *et al.* 1982; Bridle and Perley 1983; Perley *et al.* 1984). The *average* collimation behavior of 18 extragalactic radio jets whose transverse widths have been measured at several distances from their parent objects is summarized in Table III. This table gives the mean lateral expansion rate (or "spreading rate"—the term com-

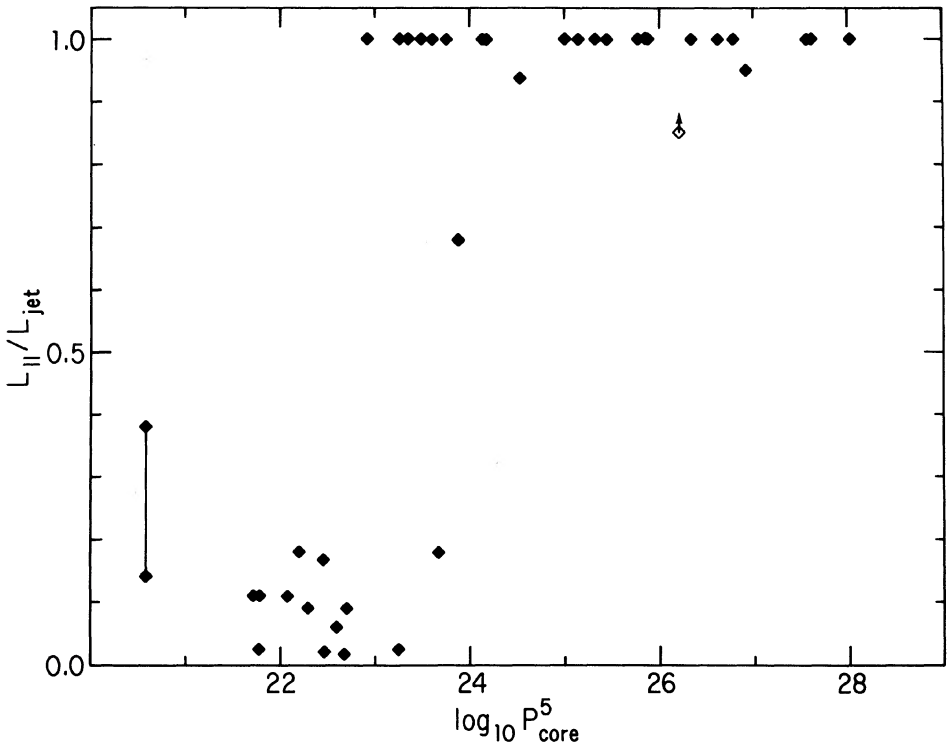

FIG. 2. Change in dominant jet magnetic field configuration with increasing core power, from the data in Table II. $L_\parallel$ is the length of the (initial) segment of the jet over which the field is aligned predominantly parallel to the jet axis; L_j is the total length of the jet. The open symbol represents a lower limit to $L_\parallel/L_j$ for the source 1258 + 40, in which the linearly polarized signal cannot be detected all along the jet, but the field is parallel to the jet axis over the entire detectable region. The barred symbol represents an ambiguity (due to an anomalously polarized knot) in defining the field transition point for the jet in the radio galaxy 1137 + 18; the data for this source are plotted despite this ambiguity, as it has the weakest core in this group.

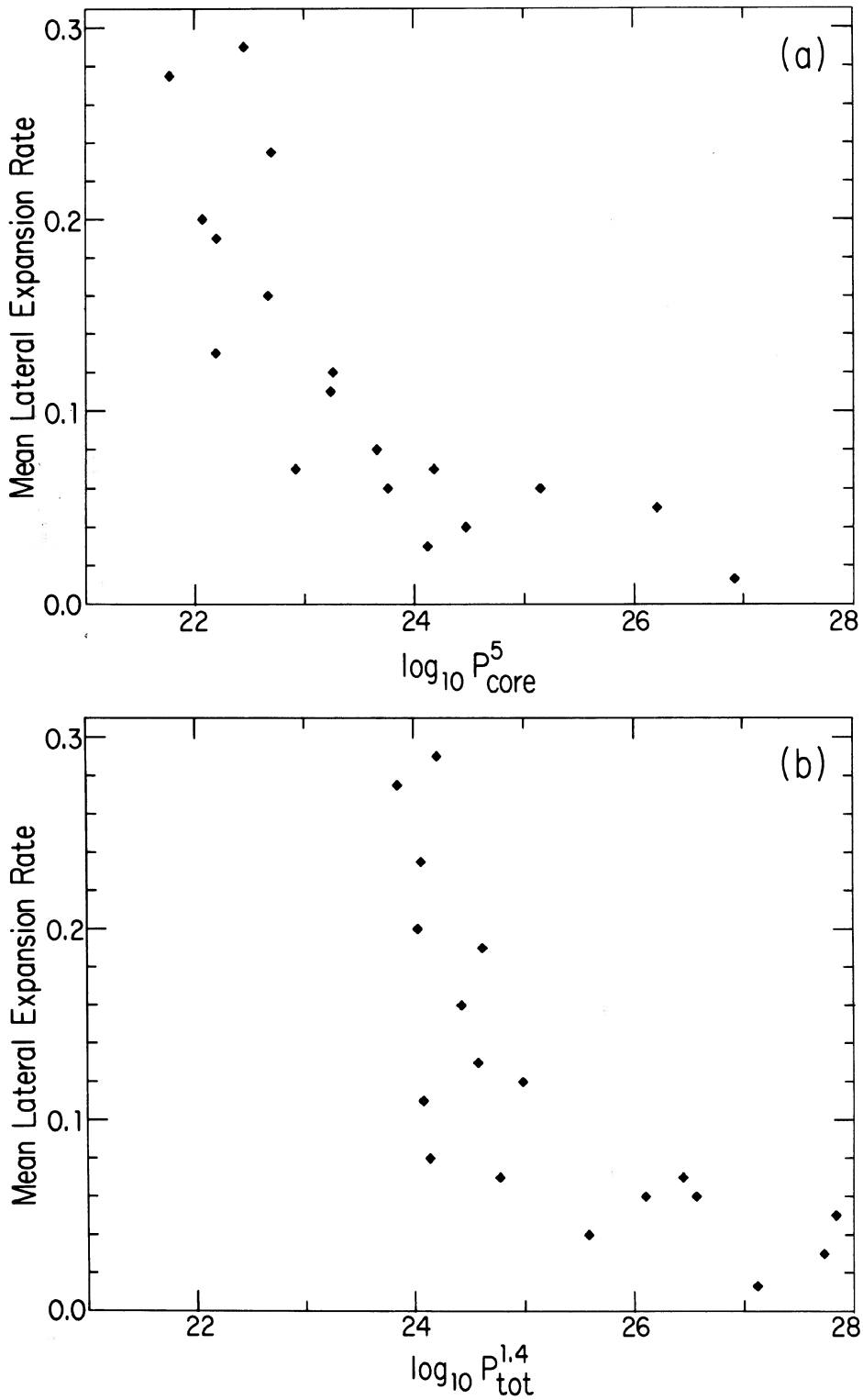

FIG. 3. Decrease in spreading rates of resolved jets in sources of increasing (a) core power at 5 GHz, (b) total power at 1.4 GHz. The mean lateral expansion (spreading) rates are tabulated in Table III.

mon in fluid mechanics) derived as the ratio of the radio FWHM Φ (deconvolving the instrumental beamwidth) to the angular distance Θ from the core halfway along the jet. The expansion rates for jets and their counterjets have been averaged (they are generally within about 20% of each other).

b) Collimation and Source Power

Figure 3(a) plots the collimation data from Table III against the 5-GHz core power for each source; Fig. 3(b) plots them against the 1.4-GHz total source power. The mean lateral expansion rates of resolved jets in the sources with 5-GHz core powers $< 10^{23.5}$ W/Hz are generally greater than those in sources with stronger cores. This trend is clearer when 1.4-GHz total power is the independent variable, as in Fig. 3(b); the resolved jets in sources with 1.4-GHz total powers $< 10^{25}$ W/Hz expand more rapidly than those in the more powerful sources.

c) Possible Biases

Is there an observational bias against finding equally rapidly widening jets in the more powerful sources? To answer this, consider first the resolution effects in sources of different powers. The more powerful sources in samples of similar radio flux density are more distant, so smaller beamwidths are required to resolve a given transverse linear scale in these sources than in their less powerful counterparts. However, if the spreading rates were actually similar for all jets, observations *with similar numbers of beamwidths along the jets* would reveal their lateral expansions equally easily whatever the total source power (providing the jet itself is detected). Many jets in the powerful sources in Fig. 3 have, in fact, been observed with as many beamwidths along their lengths as those in the weaker sources, so the trend shown there is *not* likely to be due solely to resolution bias.

Second, consider surface-brightness effects. Rapidly expanding *laminar* flows will dim rapidly with distance from the core if their particles and fields expand adiabatically (e.g., Perley *et al.* 1984). They would fade quickly and thus be hard to recognize as jets. The rapidly widening jets in weak sources dim at very subadiabatic rates, however (e.g., Burch 1979; Bridle *et al.* 1980; Willis *et al.* 1981; Bridle 1982), suggesting that the direct effects of lateral expansion in such jets are compensated by particle reacceleration, deriving its energy from the bulk kinetic energy of the flow (BP). Rapidly expanding jets in strong sources might therefore be harder to detect than similar jets in weak sources if the jet flows in powerful sources were laminar rather than turbulent. This is not the case in practice, however, as there is no hint of conical jet-like structures even in low-resolution maps of most of the powerful "unjetted' sources. Furthermore, the lobes of the powerful sources often contain compact "hot spots;" if these are interpreted as Mach disks at the ends of jets, their small diameters suggest that the "invisible" flows powering strong unjetted sources are as well collimated as the "visible" jets in the powerful sources plotted in Fig. 3b.

It is therefore unlikely that the lack of known *rapidly expanding* jets in powerful sources is due merely to observational selection.

d) Commentary

As only about 15% of all known extragalactic jets have yet been resolved transversely, Figs. 3(a) and 3(b) may trace upper envelopes to the true distribution of expansion rates with source power. The trends in these figures should therefore be re-evaluated when more complete samples of transverse resolved jets are available. The approximate dependence of the upper envelope of the lateral expansion rates against total power is $P_{\rm tot}^{-0.25}$.

V. DISCUSSION

The above data show that jets in sources with core powers below about 10^{23}–$10^{23.5}$ W/Hz at 5 GHz are generally two sided and dominated by perpendicular magnetic fields on-axis; those whose lateral expansion rates are known generally widen rapidly. Those in sources with core powers above about $10^{23.5}$–10^{24} W/Hz at 5 GHz are generally one sided, dominated by parallel fields, and widen more slowly. These transitions in jet properties also correspond to total source powers near 10^{25} W/Hz at 1.4 GHz in most cases. Although the three jet samples used here are not "complete" in the statistical sense, they are not biased in ways which would fabricate such trends. It is therefore becoming important to identify what property of the sources that changes with power produces these systematic trends in the properties of their jets.

The large-scale structures of the extended sources also change character at about the same total power as the major transitions in the jet properties. The transition from dominantly edge-darkened large-scale structures—Class I of Fanaroff and Riley (1974, hereafter referred to as FR)—to dominantly edge-brightened (FR Class II) occurs at 1.4-GHz total powers near 10^{25} W/Hz in the BP sample of 125 jetted sources. Thus the rapidly expanding, two-sided jets dominated by perpendicular fields tend to feed edge-darkened structures without prominent hot spots, whereas narrow, one-sided jets dominated by parallel fields tend to feed edge-brightened structures with (at least in the more powerful cases) prominent hot spots.

Note that the changes in these characteristics of the detected radio jets appear to be related to core and total radio powers rather than to the optical luminosity of the parent object (i.e., whether it is a radio galaxy or a quasar). Although all well-observed jets in QSR's are narrow, one sided, and dominated by a parallel magnetic field, the jets in radio galaxies may be of either type, depending on their radio power. The properties of the detected radio jets in galaxies with total radio powers $> 10^{25}$ W/Hz at 1.4 GHz are very similar to those of the detected jets in extended QSR's of comparable radio power. Recent studies of some complete samples of distant radio sources (reviewed in BP) show, however, that detectable jets are much *rarer* in strong radio galaxies than in QSR's with similar radio powers. BP argue that the detectability of jets in such powerful sources may be related to the relative prominence of their radio cores. This may, in turn, be related to the relative prominence of the optical nucleus, and thus to whether the object is termed a radio galaxy or a quasar.

The correlations described here were not predicted by any of the established models for energy transport in extragalactic radio sources. Indeed, they have yet to be incorporated into such models convincingly, and thus do not favor any one model. It is clear, however, that modelers should now attempt to identify which physical parameters of jets (velocity, Mach number?) vary with total and core radio power to produce these correlations, and why.

I thank many colleagues who provided maps of radio jets in advance of publication, and who are named individually in the table of 125 jets in the review by BP. I also thank Jack Burns, Dick Henriksen, Rick Perley, and Craig Walker for helpful discussions.

REFERENCES

Bridle, A. H. (1982). In *Extragalactic Radio Sources*, Proceedings of IAU Symposium No. 97, edited by D. S. Heeschen and C. M. Wade (Reidel, Dordrecht), p. 121.

Bridle, A. H. Henriksen, R. N., Chan, K. L., Fomalont, E. B., Willis, A. G., and Perley, R. A. (1980). Astrophys. J. Lett. **241**, L145.

Bridle, A. H., and Perley, R. A. (1983). In *Astrophysical Jets*, Proceedings of an International Workshop, edited by A. Ferrari and A. G. Pacholczyk (Reidel, Dordrecht), p. 57.

Bridle, A. H., and Perley, R. A. (1984). Annu. Rev. Astron. Astrophys. **22**, 319. (BP)

Burch, S. F. (1979). Mon. Not. R. Astron. Soc. **187**, 187.

Burns, J. O., Basart, J. P., De Young, D. S., and Ghiglia, D. C. (1984). Astrophys. J. (in press).

Burns, J. O., Feigelson, E. D., and Schreier, E. J. (1983). Astrophys. J. **273**, 128.

Cornwell, T. J., and Perley, R. A. (1982). In *Extragalactic Radio Sources, Proceedings of IAU Symposium No. 97*, edited by D. S. Heeschen and C. M. Wade (Reidel, Dordrecht), p. 139.

Fanaroff, B. L., and Riley, J.M. (1974). Mon. Not. R. Astron. Soc. **167**, 31P.

Pearson, T. J., and Readhead, A. C. S. (1984). Annu. Rev. Astron. Astrophys. **22** (in press).

Perley, R. A., Bridle, A. H., and Willis, A. G. (1984). Astrophys. J. Suppl. **54**, 291.

Saunders, R., Baldwin, J. E., Pooley, G. G., and Warner, P. J. (1982). Mon. Not. R. Astron. Soc. **197**, 287.

Schwab, F. R. (1980). SPIE J. **231**, 18.

Strom, R. G., Fanti, R., Parma, P., and Ekers, R. D. (1983). Astron. Astrophys **122**, 305.

Willis, A. G., Strom, R. G., Bridle, A. H., and Fomalont, E. B. (1981). Astron. Astrophys. **95**, 250.